

Synthesis and Biological Characterization of 1-Methyl-1,2,5,6-tetrahydropyridyl-1,2,5-thiadiazole Derivatives as Muscarinic Agonists for the Treatment of Neurological Disorders

Yang Cao,[†] Minjia Zhang,[†] Cindy Wu,[†] Selina Lee,[†] Mary Elizabeth Wroblewski,[†] Trisha Whipple,[†] Peter I. Nagy,[†] Krisztina Takács-Novák,[‡] Attila Balázs,[§] Szilárd Törös,[§] and William S. Messer, Jr.*[†]

Departments of Medicinal & Biological Chemistry and Pharmacology, College of Pharmacy, The University of Toledo, 2801 West Bancroft Street, Toledo, Ohio 43606, Institute of Pharmaceutical Chemistry, Semmelweis University, Högyes E. u. 9, H-1092 Budapest, Hungary, and Department of Organic Chemistry, University of Veszprem, Wartha V. u. 1., H-8200 Veszprem, Hungary

Received March 14, 2003

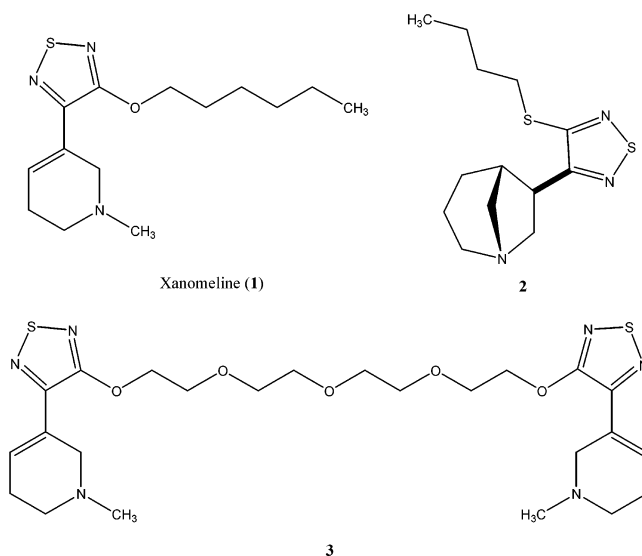
Muscarinic agonists might be useful in the treatment of neurological disorders, including Alzheimer's disease, schizophrenia, chronic pain, and drug abuse. Previous studies identified a series of bis-1,2,5-thiadiazole derivatives of 1,2,5,6-tetrahydropyridine with high activity and selectivity for muscarinic receptors. To develop compounds with improved central nervous system penetration, several new derivatives were synthesized and characterized for muscarinic receptor binding and activity. One ligand (**11**) exhibited agonist activity at M₁, M₂, and M₄ receptors, a selectivity profile suggesting potential utility in the treatment of schizophrenia.

Introduction

Muscarinic receptors belong to the super family of G protein-coupled receptors, and mediate many of the actions of acetylcholine throughout the brain and peripheral tissues. Five muscarinic receptor subtypes have been identified and characterized using a variety of pharmacological and molecular biological techniques.¹

Several lines of evidence have suggested that selective muscarinic agonists could be useful in the treatment of schizophrenia. Anticholinergic drugs, including the glycolate esters, produce psychotomimetic effects in humans.² High doses of muscarinic antagonists used in the treatment of Parkinson's disease (e.g., benztrapine, trihexyphenidyl) produce hallucinations and confusion. In contrast, Alzheimer's disease patients treated with cholinesterase inhibitors, which elevate levels of acetylcholine, exhibit improvements in neuropsychiatric symptoms such as agitation, hallucinations, and psychosis.^{3–5} In addition, the selective M₁ muscarinic agonist xanomeline (**1**) significantly improved psychiatric symptoms such as hallucinations in phase II clinical trials in Alzheimer's patients.⁶ Unfortunately, xanomeline produced unwanted side effects associated with activation of M₃ receptors, including salivation, diarrhea, and profuse sweating, which limited patient compliance.⁷

Follow-up preclinical studies with structurally related compounds identified strong antipsychotic activity in (5*R*,6*R*)-6-(3-butylthio-1,2,5-thiadiazol-4-yl)-1-azabicyclo[3.2.1]octane (**2**), which displays partial agonist activity at M₂ and M₄ receptors.⁸ Compounds **1** and **2** may exert an antipsychotic action by regulating the release of dopamine in the frontal cortex. Compounds **1** and **2**



produce very few of the adverse side effects (e.g., catalepsy) associated with classical antipsychotics such as haloperidol, suggesting that selective muscarinic agonists might provide a useful alternative therapeutic approach to treating the symptoms of schizophrenia. Moreover, muscarinic agonists might be particularly useful in improving cognitive function (including memory function, language use, and constructional praxis) in schizophrenic patients.⁹ A key factor in developing muscarinic agonists as antipsychotics will be limiting the side effects associated with M₃ receptor activation.

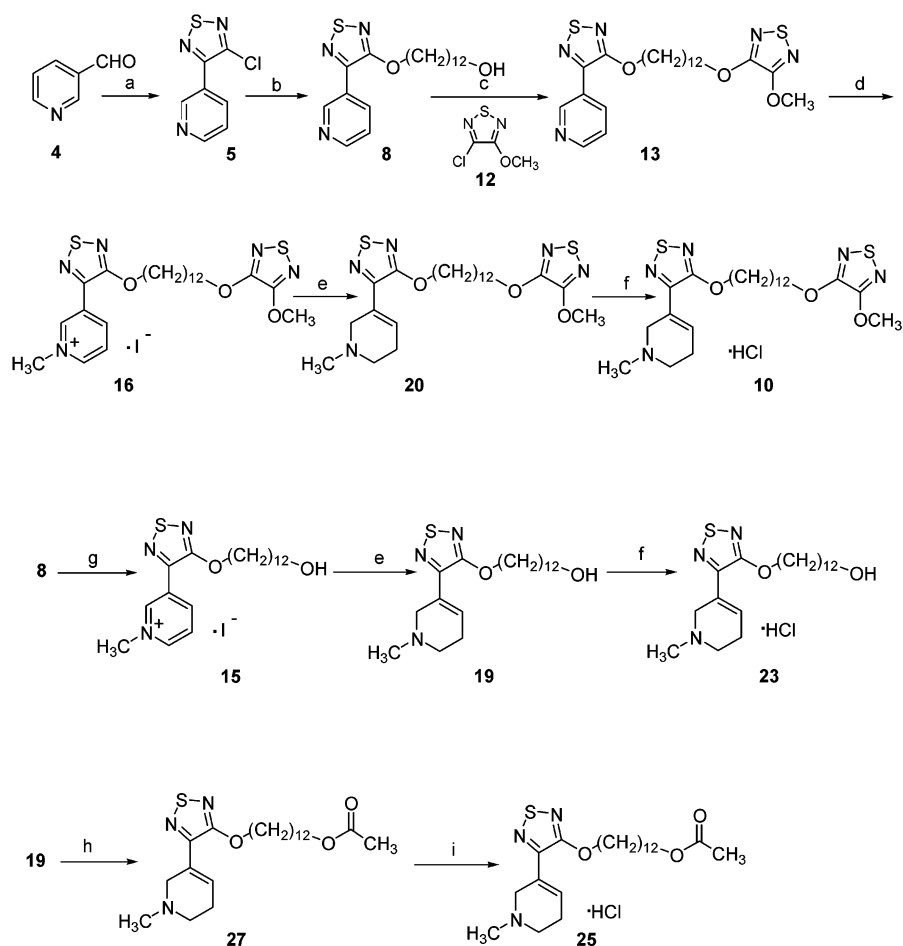
Behavioral studies of muscarinic receptor knockout mice highlight the potential utility of selective M₁ and M₄ agonists in the treatment of psychosis.¹⁰ For example, M₄ receptors modulate locomotor activity produced by the stimulation of D₁ dopamine receptors. M₄ knockout mice also show enhanced sensitivity to the effects of phencyclidine on the prepulse inhibition model of psychosis. M₁ agonists might be particularly useful

* To whom correspondence should be addressed. Tel: 419-530-1958. Fax: 419-530-1909. E-mail: wmesser@utnet.utoledo.edu.

[†] The University of Toledo.

[‡] Semmelweis University.

[§] University of Veszprem.

Scheme 1^a

^a (a) KCN/H₂O/HOAc, NH₄Cl/NH₃(aq), S₂Cl₂/DMF. (b) HO(CH₂)₁₂OH (**6**), NaH, THF, reflux. (c) Compound **12**, NaH, THF, reflux. (d) CH₃I, acetone, room temperature. (e) NaBH₄, CH₃OH/CHCl₃, 0–5 °C. (f) HCl(g), CH₃OH/CHCl₃, 0–5 °C. (g) CH₃I, acetone/CHCl₃, room temperature. (h) Ac₂O, ZnCl₂, 85 °C. (i) 1 M HCl/ether, acetone/ether, 0–5 °C.

Chart 1

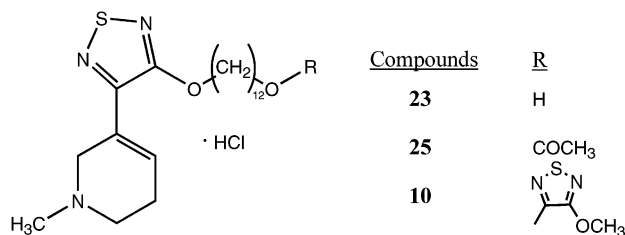
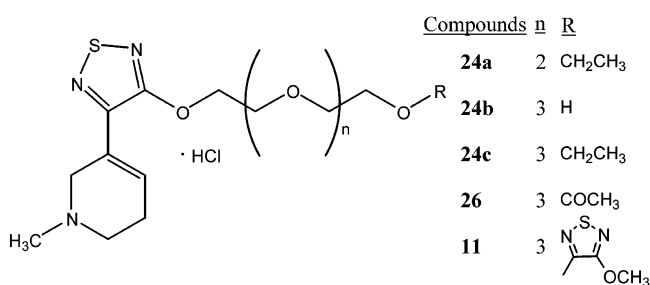


Chart 2

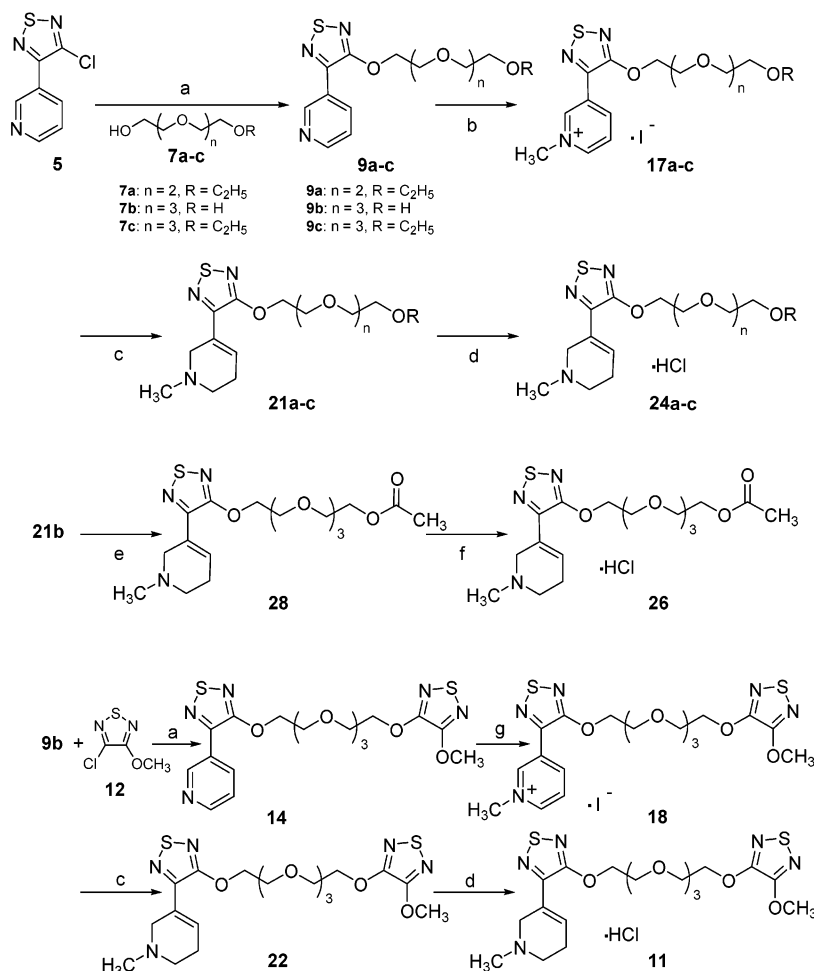


in treating memory and cognitive deficits associated with schizophrenia.⁹ Taken together, the data suggest a role for M₁/M₄ agonists in the treatment of schizophrenia.

The clinical utility of muscarinic agonists for the treatment of schizophrenia has not been adequately

assessed due to the lack of compounds exhibiting an appropriate combination of agonist activity and selectivity for M₁/M₄ receptors. Recently, a novel series of bivalent ligands was developed with strong agonist activity at M₁ and M₄ receptors and very low activity at M₃ and M₅ receptors.¹¹ Among the compounds, **3** displayed high potency and agonist activity at M₁ receptors. However, the inherent weaknesses associated with the structural features of bivalent ligands (relatively large size, hydrophobicity of alkyl linking groups, and the presence of two basic amines in one molecule) likely limit membrane permeability and bioavailability. The subtype selectivity of bivalent ligands may derive from interactions with nonconserved residues within the extracellular domains of muscarinic receptors. The hypothesized mechanism of agonist activation calls for the tetrahydropyridyl group penetrating into the binding pocket formed by Asp105, Thr192, and Asn382 residues, while the polar group at the other end of the bivalent ligand interacts with the extracellular loops. To explore whether the bivalent ligand is flexible enough to take the required conformation from the one adopted in the biological fluid within the synaptic cleft, molecular dynamics (MD) calculations were performed in the present studies.

To develop selective muscarinic agonists with therapeutic potential, two new series of tetrahydropyridyl

Scheme 2^a

^a (a) NaH, THF, reflux. (b) CH_3I , acetone/ $CHCl_3$, room temperature. (c) $NaBH_4$, $CH_3OH/CHCl_3$, 0–5 °C. (d) HCl(g), $CH_3OH/CHCl_3$, 0–5 °C. (e) Ac_2O , $ZnCl_2$, 85 °C. (f) 1 M HCl/ether, 0–5 °C. (g) CH_3I , acetone, room temperature.

thiadiazole derivatives were designed. Three compounds were synthesized in the series of tetrahydropyridyl thiadiazole derivatives with an alkyl linker (see Chart 1), while five compounds were synthesized with a poly(ethylene glycol) linker (see Chart 2). MD simulations also examined the structural consequences of replacing a cationic tetrahydropyridyl–thiadiazole moiety with different neutral groups. One compound (**11**) displayed robust agonist activity at M_1 , M_2 , and M_4 receptors suggesting potential utility in the treatment of psychiatric disorders.

Results and Discussion

Chemistry. As shown in Schemes 1 and 2, the starting material 3-(3-chloro-1,2,5-thiadiazol-4-yl)pyridine (**5**) was synthesized from 3-pyridinecarboxaldehyde (**4**) following published procedures.¹² Tetra(ethylene glycol) monoethyl ether (**7c**) was prepared from the reaction of tetra(ethylene glycol) (**7b**) with NaH and $BrCH_2CH_3$ in tetrahydrofuran (THF) in a yield of 25.5%. 4-Chloro-3-methoxy-1,2,5-thiadiazole (**12**) was synthesized in 10.1% yield by reacting 3,4-dichloro-1,2,5-thiadiazole (**29**) with $NaOCH_3$. Compound **5** was reacted with 1,12-dodecanediol (**6**), tri(ethylene glycol) monoethyl ether (**7a**), **7b**, or **7c** in the presence of NaH in refluxing THF to give mono-[3-(pyrid-3-yl)-1,2,5-thiadiazol-4-yl] ethers (compounds **8** and **9a–c**) in 41.7–

95.3% yield. The ethers were treated with excess CH_3I to yield the quaternary ammonium iodides (compounds **15** and **17a–c**) in 91.5–99.7% yield. The quaternary salts then were treated with 4 equivalents of $NaBH_4$ in CH_3OH and $CHCl_3$ to give the free bases (compounds **19** and **21a–c**). Then, dry HCl gas was used to convert the purified free bases into their corresponding hydrochloride salts (**23** and **24a–c**) in 46.2–76.9% yield.

For **10** and **11**, prior to quaternization, the resulting 12-[3-(pyrid-3-yl)-1,2,5-thiadiazol-4-yloxy]-1-dodecanol (**8**) and tetra(ethylene glycol) mono-[3-(pyrid-3-yl)-1,2,5-thiadiazol-4-yl] ether (**9b**) were reacted further with **12** to give compounds **13** and **14** in 26.6 and 41.9% yield, respectively. The corresponding quaternary ammonium iodides **16** and **18** were obtained in 81.8 and 98.4% yield, which were converted into their hydrochloride salts **10** and **11** in 65.3 and 16.1% yield, respectively, following $NaBH_4$ reduction and treatment with hydrogen chloride gas.

For **25** and **26**, the free bases (**19** and **21b**) were transformed to the corresponding acetyl esters (compounds **27** and **28**) by reacting with excess acetic anhydride in the presence of catalytic anhydrous $ZnCl_2$ before conversion into hydrochloride salts. Etheral HCl then was added into the methylene chloride solution of compounds **27** or **28**. After crystallization from acetone/

Table 1. Pharmacological Properties of Novel Compounds at M₁ Receptors Expressed in A9 L Cells^a

	M ₁ receptors		
	pK _i	pEC ₅₀	S _{max}
carbachol	5.5 ± 0.13	5.5 ± 0.17	1500 ± 300
1	6.8 ± 0.01	8.0 ± 0.04	770 ± 120
3	10 ± 0.23	8.1 ± 0.05	960 ± 81
10	5.7 ± 0.10	6.4 ± 0.15	500 ± 13
11	7.6 ± 0.26	7.2 ± 0.13	600 ± 56
23	7.3 ± 0.56	5.5 ± 0.03	250 ± 29
24a	6.2 ± 0.13	nd	nd
24b	7.1 ± 0.24	6.2 ± 0.10	240 ± 64
24c	6.4 ± 0.25	5.2 ± 0.77	420 ± 220
25	8.4 ± 0.64	5.6 ± 0.19	280 ± 17
26	6.7 ± 0.26	nd	nd

^a Data include the inhibition of [³H]-(*R*)-QNB binding and stimulation of phosphoinositide metabolism. Data represent the mean ± SEM from at least two assays, each performed in triplicate; nd, not determined.

Table 2. Pharmacological Properties of Novel Compounds at M₂ Receptors Expressed in A9 L Cells^a

	M ₂ receptors		
	pK _i	pIC ₅₀	I _{max} (%)
carbachol	7.0 ± 0.21	7.9 ± 0.23	65 ± 4.3
1	7.3 ± 0.15	nc	na
3	9.9 ± 0.25	9.2 ± 0.29	92 ± 18
10	7.8 ± 0.26	nd	nd
11	8.1 ± 0.02	9.3 ± 0.30	76 ± 4.8
23	7.8 ± 0.21	nd	nd
25	7.8 ± 0.25	nd	nd

^a Data include the inhibition of [³H]-(*R*)-QNB binding and inhibition of cAMP formation. Data represent the mean ± SEM from at least three assays, each performed in triplicate; na, no significant change from basal levels; nc, not calculable due to inconsistent dose response curves from assay to assay; nd, not determined.

Table 3. Pharmacological Properties of Novel Compounds at M₃ Receptors Expressed in A9 L Cells^a

	M ₃ receptors		
	pK _i	pEC ₅₀	S _{max}
carbachol	5.2 ± 0.24	4.7 ± 0.23	350 ± 48
1	7.1 ± 0.07	4.6 ± 0.34	280 ± 43
3	8.3 ± 0.28	nc	na
10	7.1 ± 0.17	3.4 ± 0.39	50 ± 5.6
11	7.6 ± 0.06	nc	na
23	7.1 ± 0.10	5.0 ± 0.39	73 ± 12
25	6.9 ± 0.14	4.4 ± 0.16	200 ± 28

^a Data include the inhibition of [³H]-(*R*)-QNB binding and stimulation of phosphoinositide metabolism. Data represent the mean ± SEM from at least two assays, each performed in triplicate; na, no significant change from basal levels; nc, not calculable due to inconsistent dose response curves from assay to assay.

ether, the final compounds **25** and **26** were obtained in 36.3–48.0% yield.

Pharmacology. Compounds were initially examined for receptor binding properties and abilities to stimulate biochemical responses in cell lines expressing muscarinic receptor subtypes. Ligand binding affinities (pK_i values) were determined by measuring the inhibition of specific [³H]-(*R*)-QNB (quinuclidinyl benzilate) binding to human muscarinic receptor subtypes expressed in A9 L cells and compared with carbachol, **1**, and **3** (see Tables 1–5). In general, the tetrahydropyridyl thiazadiazole derivatives inhibited the binding of [³H]-(*R*)-QNB in a dose-dependent manner with pK_i values ranging from 5.7 to 8.6. Compound **25** displayed the highest affinity for M₁ receptors with a pK_i of 8.4. Among the

Table 4. Pharmacological Properties of Novel Compounds at M₄ Receptors Expressed in A9 L and CHO Cells^a

	M ₄ receptors		
	pK _i	pIC ₅₀	I _{max}
carbachol	6.4 ± 0.26	6.0 ± 0.38	50 ± 10
1	7.4 ± 0.05	7.6 ± 0.18	39 ± 5.9
3	8.7 ± 0.05	nd	nd
10	7.7 ± 0.10	nd	nd
11	8.6 ± 0.12	7.8 ± 0.50	20 ± 5.4
23	7.5 ± 0.12	nd	nd
25	7.1 ± 0.08	nd	nd

^a Data include the inhibition of [³H]-(*R*)-QNB binding (from A9 L cells) and inhibition of cAMP formation (from CHO cells). Data represent the mean ± SEM from at least two assays, each performed in triplicate; nd, not determined.

ligands, compound **11** displayed the highest affinity for M₂, M₃, and M₄ receptors with pK_i values of 8.1, 7.6, and 8.6, respectively (see Figure 1). Compound **23** displayed the highest affinity for M₅ receptors with a pK_i of 6.9. None of the compounds exhibited marked selectivity for a single muscarinic receptor subtype in terms of binding affinity, although all compounds displayed relatively low affinity for M₅ receptors.

Agonist activity was assessed by measuring phosphoinositide metabolism in A9 L cells expressing M₁, M₃, and M₅ receptors and by assaying cAMP levels in A9 L and Chinese hamster ovary (CHO) cells expressing M₂ and M₄ receptors, respectively (see Tables 1–5). Compound **11** displayed the highest activity at M₁ receptors, with a pEC₅₀ of 5.7 and a maximal response of 40% of that of carbachol (see Figure 2). Compound **11** was essentially inactive at M₃ receptors and displayed very low potency (pEC₅₀ of 3.7) and activity (14% of the carbachol response) at M₅ receptors. Of the compounds tested, **25** displayed the highest activity at M₃ receptors (57% of the carbachol response), while **26** displayed the highest activity at M₅ receptors (28% of the carbachol response). On the basis of the phosphoinositide metabolism data, compound **11** would not be expected to produce peripheral side effects (e.g., salivation, lacrimation, and diarrhea) associated with activation of M₃ receptors, which are present in smooth muscle and exocrine glands.

Agonist activity also was assessed by measuring the ability of selected compounds to inhibit the formation of cAMP stimulated by forskolin in A9 L cells expressing M₂ receptors and in CHO cells expressing M₄ receptors. Compound **11** displayed strong M₂ agonist activity (76% inhibition with a pIC₅₀ of 9.3) as shown in Figure 3A and Table 2. Carbachol was slightly less efficacious and less potent (65% inhibition with a pIC₅₀ of 7.9). All responses were blocked by addition of the muscarinic antagonist *l*-hyoscyamine (data not shown). Compound **11** also displayed partial agonist activity at M₄ receptors expressed in CHO cells (see Figure 3B and Table 4). On the basis of the adenylyl cyclase activity data, compound **11** would be expected to produce hypothermia through activation of central M₂ receptors.

In pharmacological screens in mice, M₃ receptor-mediated side effects (i.e., diarrhea, salivation, and lacrimation) were minimal for compound **11** at doses up to 10 mg/kg i.p. (data not shown). The in vivo data for compound **11** are consistent with a lack of efficacy at M₃ receptors expressed in A9 L cells. In contrast, xanomeline produces diarrhea, salivation, and lacrima-

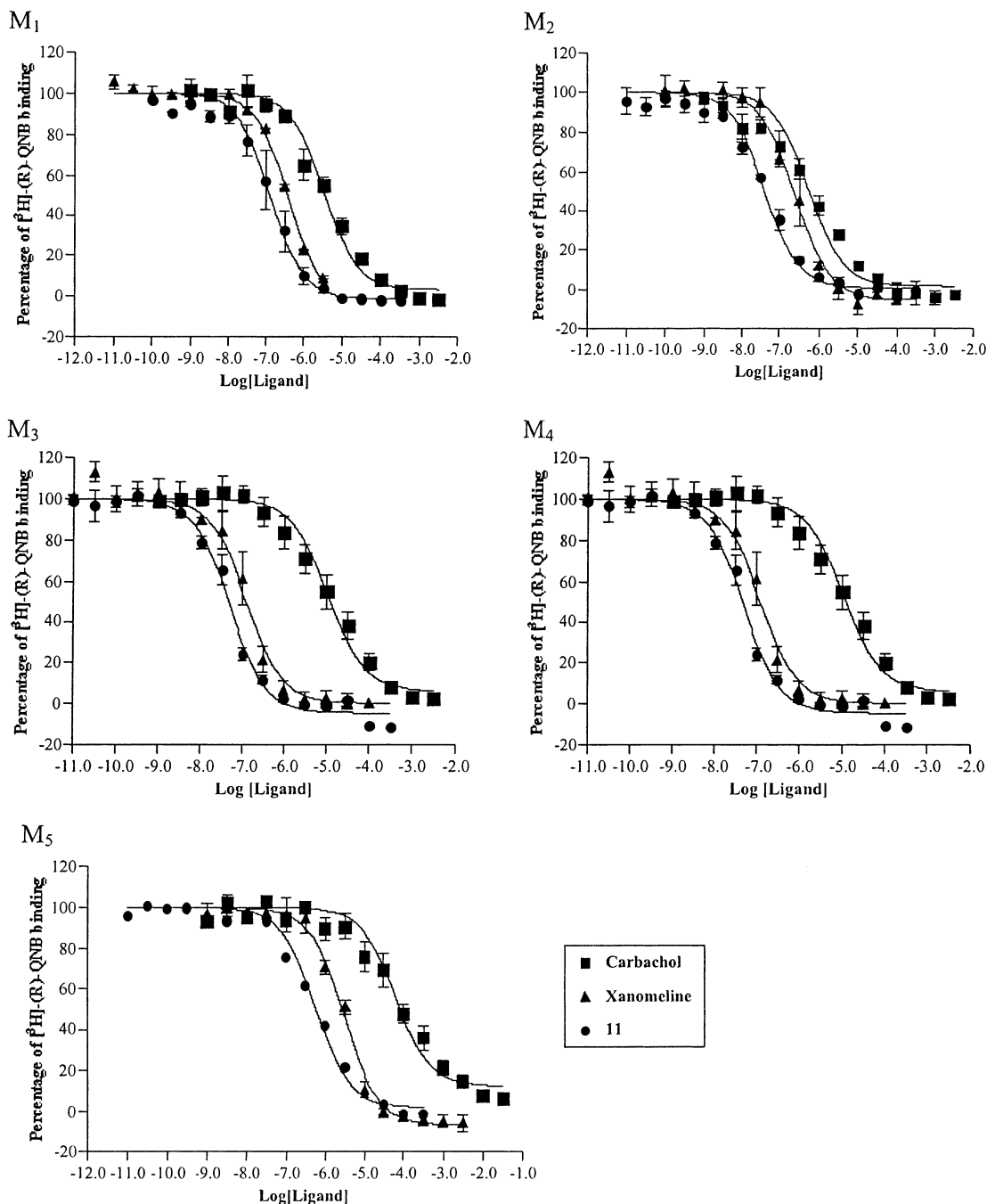


Figure 1. Inhibition of [³H]-(R)-QNB binding to muscarinic receptor subtypes expressed in A9 L cells by carbachol, **1**, and **11**. Data represent the mean \pm SEM from a minimum of three assays, each performed in triplicate.

tion at 1.0 and 10 mg/kg i.p.¹³ Compound **11** did produce slight tremors and induced hypothermia (see Figure 4), consistent with activity at central M₂ receptors. Taken together, the in vivo data suggest that compound **11** is able to penetrate into the brain and act as an agonist at M₂ receptors involved in regulating movement and body temperature. Substantial M₂ effects were only seen at the highest dose.

Ex vivo binding studies were conducted to examine the ability of **11** to cross the blood–brain barrier. Rats were injected with either saline, **11**, or oxotremorine (both at doses of 0.1 or 1.0 mg/kg, i.p.) and sacrificed at either 30 or 60 min following injections. The brain was removed rapidly, and membranes were prepared for receptor binding assays. Displacement of [³H]QNB binding was assessed in treated animals as compared

to saline-injected controls, and the results were expressed as the percentage inhibition of specific [³H]QNB binding. Both **11** and oxotremorine inhibited [³H]QNB binding in a dose-dependent manner, as shown in Figure 5. Oxotremorine inhibited [³H]QNB binding at both 30 and 60 min, while **11** inhibited [³H]QNB binding only at 30 min. Thus, compound **11** appears to penetrate readily into the brain at doses that produce minimal peripheral side effects.

The pharmacological profile of compound **11** suggests potential utility in the treatment of schizophrenia. Compound **11** acted as an agonist at both M₂ and M₄ receptors, which may play important roles in regulating dopamine release in the central nervous system. In addition, **11** activated M₁ receptors, which play a role in memory and cognitive function, suggesting potential

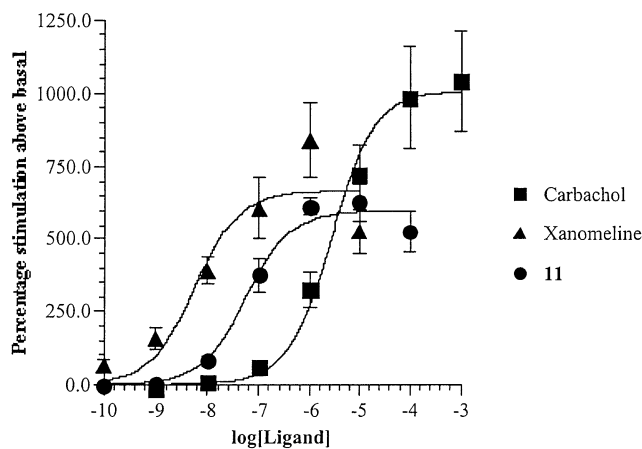


Figure 2. PI hydrolysis mediated by carbachol, **1**, and **11** through human M_1 receptors expressed in A9 L cells. Data represent the mean \pm SEM from a minimum of three assays, each performed in triplicate.

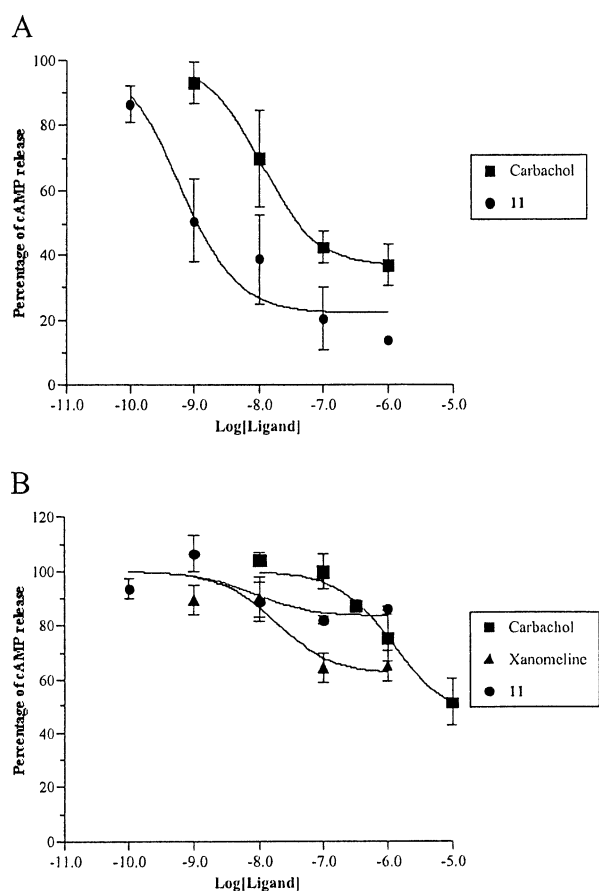


Figure 3. Inhibition of forskolin-stimulated cAMP formation mediated by carbachol and **11**. (A) Inhibition of cAMP formation through human M_2 receptors expressed in A9 L cells. (B) Inhibition of cAMP formation through human M_4 receptors expressed in CHO-K1 cells. Data represent the mean \pm SEM from a minimum of three assays, each performed in triplicate.

utility in treating cognitive deficits associated with schizophrenia. The lack of activity at M_3 receptors suggests that compound **11** should have a low side effect profile, particularly with respect to salivation, lacrimation, and diarrhea. In addition, **11** did not activate M_5 receptors yet bound with reasonable affinity. Because M_5 receptors promote dopamine release, the ability to block M_5 receptors may provide an additional advantage

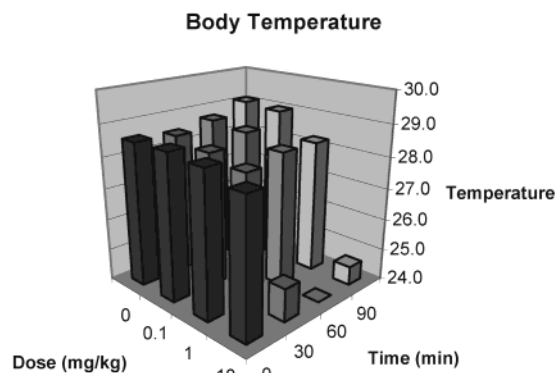


Figure 4. Hypothermia produced by **11** following i.p. administration in mice. Data represent the mean core body temperature (in $^{\circ}\text{C}$) of mice.

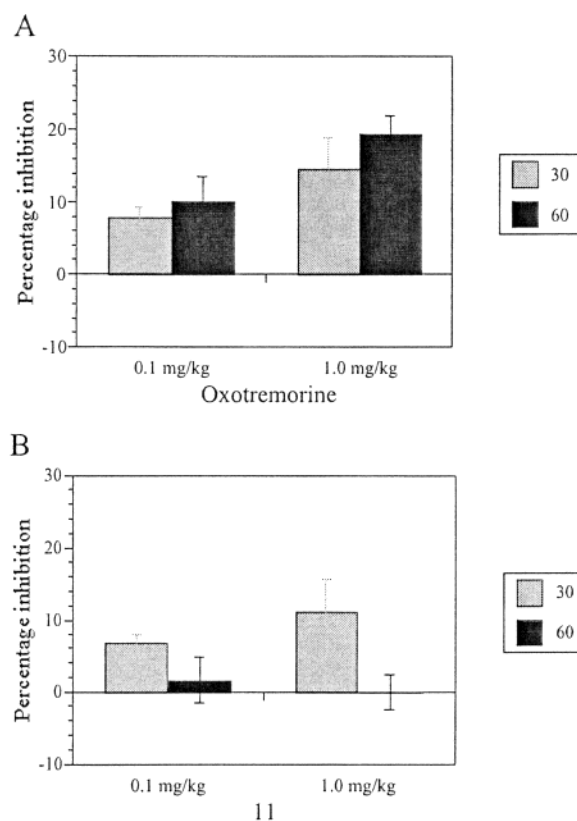


Figure 5. Inhibition of [^3H]QNB binding to rat brain by oxotremorine (A) and **11** (B) following i.p. injections. Data represent the mean \pm SEM from a minimum of three animals for each dose and time point (30 and 60 min).

for **11** in the treatment of schizophrenia or even drug abuse. Additional studies are necessary to assess the activity of **11** in peripheral tissues to verify the selectivity profile found in cell lines.

Computational Chemistry. Molecular modeling of molecules can help reveal important structural features for consideration in studying the possible binding and activation mechanisms of muscarinic agonists. Acetylcholine, the natural agonist for muscarinic receptors, is subject only to limited conformational flexibility. Acetylcholine is a small molecule, and its conformation can be primarily characterized with gauche or trans N-C-C-O arrangements. As a neurotransmitter, acetylcholine diffuses from presynaptic neurons through an extracellular solution into the binding cavity of receptors on either pre- or postsynaptic neurons.

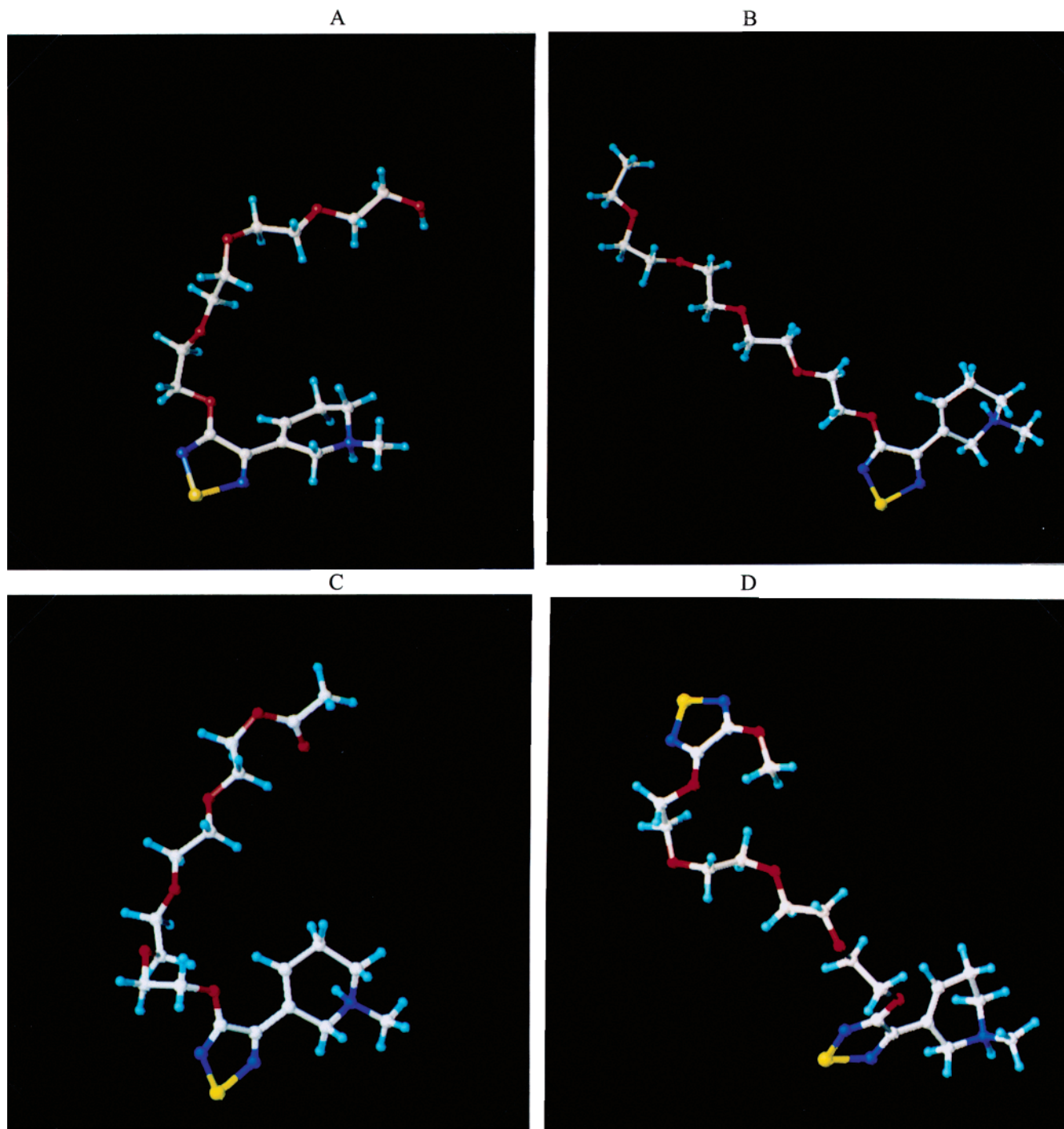


Figure 6. Conformations of novel compounds after 130 ps gas phase and 500 ps in solution MD calculations.

According to a recent tandem binding model,¹⁴ an acetylcholine molecule binds to the Asp99 carboxylate group as an initial binding site. The Asp99 residue is located at the junction of the third transmembrane domain and the first extracellular loop but can become exposed for binding of the ligand. Acetylcholine subsequently relocates to a more stable secondary binding site, which is Asp105 in M₁ receptors. The relocation requires a further opening of the pore among transmembrane domains 3, 5, and 6, to accommodate acetylcholine in the hypothesized binding cavity. In the Jakubik model, a second acetylcholine molecule binds to Asp99 thereby covering the opened pore.

Such a concerted mechanism is easily imaginable for a small agonist but becomes much more complicated for

a large ligand. The binding process starts in the conformation that the ligand adopts as it approaches the extracellular loops. In a previous study,¹¹ the flexibility of the spacer was analyzed based on MD simulations for bivalent dications including compound **3**. The in solution stable, horseshoe-shaped structure was docked to the first extracellular loop of the M₁ receptor model. It was found, however, that the binding energy is remarkably more negative when **3** is docked in an extended conformation into the binding pocket of the receptor. Thus, it is important to consider the possible shapes that the bivalent molecules can adopt. Their flexibility is crucial for reaching the binding pocket in an extended conformation, which may not be the lowest energy structure of the ligand. The previous

Table 5. Pharmacological Properties of Novel Compounds at M₅ Receptors Expressed in A9 L Cells^a

	M ₅ receptors		
	pK _i	pEC ₅₀	S _{max} (%)
carbachol	4.7 ± 0.28	5.2 ± 0.27	200 ± 23
1	5.8 ± 0.08	5.6 ± 0.16	92 ± 15
3	7.2 ± 0.03	nc	na
10	6.8 ± 0.29	nc	23 ± 14
11	6.4 ± 0.31	3.7 ± 2.1	27 ± 15
23	6.9 ± 0.08	nc	32 ± 20
25	6.2 ± 0.49	nc	34 ± 26
26	nd	5.9 ± 2.2	55 ± 22

^a Data include the inhibition of [³H]-(*R*)-QNB binding and stimulation of phosphoinositide metabolism. Data represent the mean ± SEM from at least two assays, each performed in triplicate; na, no significant change from basal levels; nc, not calculable due to inconsistent dose response curves from assay to assay.

Table 6. Calculated N···O₅ Distances (in Å) from MD Simulations at T = 310

compd	type	d _{min}	d _{max}	d _{ave}
3	dication	7.1	13.0	10.6 ± 1.2
		8.4	14.6	10.9 ± 1.2
24b	monocation	5.4	17.8	11.2 ± 2.8
24c	monocation	14.3	18.4	16.8 ± 0.7
26	monocation	5.7	17.2	11.0 ± 2.9
11	monocation	10.7	16.5	13.9 ± 1.3

studies were extended for **24b,c**, **26**, and **11** to include an analysis of the consequences of replacing a cationic end group with neutral groups of different polarities.

The structures after 130 ps gas phase and 500 ps in solution MD calculations differed essentially from the starting structures. All four molecules could be characterized as conformers with opened V or U shapes (see Figure 6). Table 6 compares the N···O₅ distances, including those for the dicationic compound **3**. Average distances (*d*_{ave}) were close for **3**, **24b**, and **26** and differed significantly from the value for **24c**. Such differences may not be very surprising, considering that **24c** has the only entirely nonpolar end group in the series studied. Thus, the smaller *d*_{ave} values are associated with more polar end groups.

The results from MD calculations are counterintuitive to the concept that dicationic headgroups tend to separate the most for compound **3**. In aqueous solution, however, there are counterions that can shield the cationic headgroups thereby balancing the dicationic repulsions with attractive anion–cation interactions. In fact, previous modeling studies for **3** indicated Cl[−] counterions located in close proximity to the protons of the tertiary amines. As a result, there are altogether two repulsive interactions (one dicationic, one dianionic), as compared to four favorable (cation–anion) electrostatic interactions. Furthermore, the bulky end groups exert large and favorable van der Waals interactions with each other.

In the new series of monocationic ligands, there is no electrostatic repulsion to be balanced by counterions. Accordingly, the Cl[−] counterion was found at a fairly large average distance of 14–18 Å from the proton connecting to the N-atom within the tetrahydropyridyl ring in **24b,c** and **26**. In contrast, the average Cl[−]···H⁺ distance was found to be 5.3 Å for compound **11**. For this system, however, the two thiaziazole rings stayed relatively close to each other forming a U rather than

an opened V structure, as for the other three compounds. The average S···S distance was 9.40 ± 2.45 Å, allowing the location of the Cl[−] between the rings for large and favorable van der Waals interactions. The net result of such interactions may help keep the anion close to the cationic headgroup.

Counterions and ions of NaCl molecules added to the modeling system had large effects on both the conformation and the flexibility of molecules with a 13 atom ethylene glycol spacer. In a separate MD run (using the same simulation parameters), three NaCl molecules were added to the system (for compound **11**) in order to mimic the isotonic saline concentration of 0.153 M NaCl solution. A remarkable decrease was found for the average S···S distance (4.30 ± 0.96 Å). Thus, the presence of a small excess of ions in the model leads to remarkable stabilization of some ligand conformations. When NaCl was not present in the solution, five simple conformational conversions were identified between local gauche and trans arrangements, and one trans–gauche–trans conversion was identified along the O₁–C···C–O₅ path in the last 250 ps of the MD trajectory. Not a single conversion was found, however, in the same time interval when three NaCl molecules were added to the system.

A possible explanation for such differences in conformational flexibility is that the NaCl ions create strongly bound and relatively rigid hydration spheres. Many water molecules belong to the spheres, and their translational and rotational freedom is reduced as compared to water molecules in solutions without excess NaCl. In the somewhat “frozen” ionic environment, conformational changes along the spacer become less feasible as well.

During the development of the M₁ receptor model, the receptor was placed in a water box. The Sybyl software removed water molecules that formed unfavorable contacts with receptor atoms but left the cavities and pores with the transmembrane helices filled with water. Even within a short MD run, however, most of the water molecules rapidly left the cavities and returned to the bulk water. Accordingly, neither a profound aqueous environment nor Na⁺ and Cl[−] ions are expected to surround the cationic headgroup of agonist molecules located within the transmembrane domain cavities. Consequently, molecules with long spacers (such as compound **11**) become more flexible when leaving the saline solution. At the same time, the receptor has to account for the electrostatic repulsion for the two protonated amines in **3** and the electrostatic stabilization of the protonated tetrahydropyridyl ring in each molecule.

For **3**, the average N···N distance is 11.8 ± 1.4 Å in aqueous solution,¹¹ a distance favorable for tandem binding to the Asp99 and Asp105 carboxylate groups by a single bivalent molecule. Such a binding mode would require, however, an unlikely wide opening of the pore formed by transmembrane helices 3, 5, and 6 in order to accommodate a horseshoe-shaped structure for **3** or a thermodynamically unfavorable, wormlike motion of the ligand, to avoid repulsion by the helical elements crossing this theoretical path. No such problem is present with compounds **24b,c**, **26**, and **11**, with only one protonated ring and without the possibility for a

single molecule, tandem protonated nitrogen...carboxylate interaction pair. For such molecules, however, the flexibility of the spacer is important. A flexible spacer may help compounds reach conformations allowing favorable interactions between the variable end groups and the receptor residues either in the extracellular loop or within the transmembrane helices. Such interactions may play a decisive role in receptor subtype selectivity.

Differences in the protonation constants (pK_a) may be related to variations in the spatial orientation of the molecules. Molecular flexibility appears to be a function of the chemical environment. Different pK_a values may reflect that the tertiary amine groups are more or less open to hydration and protonation, depending on the horseshoe, V, or U shape of the spacer. The pK_a values for **3** were measured as 8.44 ± 0.004 and 7.77 ± 0.004 . For a representative of the new mono-tertiary-amine molecules, **24b** was selected, and a pK_a of 8.27 ± 0.003 was found. The results should be analyzed with respect to the length of the spacer and the possible interaction of the polar end groups.

The basicity of monoamines is practically independent of the length of the chain. Ethylamine and octadecylamine ($C_{18}H_{37}NH_2$) have pK_a values of 10.65 and 10.60 at 25 °C.¹⁵ Thus, for primary amines, even if the alkyl chain folds back, basicity is not affected greatly. However, pK_a values for α - ω diamines are sensitive to the length of the spacer. The pK_a values for the first and second protonations of 1,2-diamino-ethane are 9.92 and 6.86, respectively. It is normal that the pK_a for the dication is smaller than for the monocation, since it reflects that a more acidic environment is required for the protonation of a cation. The corresponding values for the longest α - ω diamine, 1,8-diamino-octane ($H_2N-(CH_2)_8-NH_2$), found in ref 15, are 11.0 and 10.1. These values reveal interesting peculiarities for diamines: the basicity increases with a longer alkyl chain (in contrast to the nearly constant value for monoamines), and the difference of the pK_a values decreases to about 0.9 units. This finding can be explained theoretically, assuming that the two amine groups interact in 1,2-diamino-ethane. In a gauche conformation, a five-membered ring with an $H_2N \cdots^+HNH_2$ intramolecular hydrogen bond can be formed in the monocation, making the protonation of the second amino group less feasible.¹⁶ As a result, the pK_a for the dication is relatively low for 1,2-diamino-ethane. For 1,6-diamino-hexane, the pK_a values are 11.86 and 10.76 at 0 °C. Thus, the increase in basicity is not monotonic, but the trend is clear for the difference of the pK_a values. The decreasing difference indicates that the two amine groups become independent with respect to protonation, and implicitly suggests that the shape of the spacer may not be decisive.

Although a $-(CH_2)_8-$ spacer may behave differently than the long and chemically different spacer in **3**, the obtained results indicate that the protonation of **3** can be understood on the basis of the above qualitative argument. The $O-CH_2-(CH_2-O-CH_2)_3-CH_2-O$ spacer is long enough to separate the two protonation sites in any conformation, and the pK_a for the formation of the dication is smaller by about 0.7 units than that for the monocation.

It is important to notice that the (single) pK_a for **24b** is 8.27, which differs only slightly from the correspond-

ing pK_a value for monocationic **3**. The difference, however, is significant considering the very small standard deviations (no more than 0.004) for the two molecules. In principle, the alcoholic end group in **24b** may get close to the tertiary amine and, through formation of an intramolecular hydrogen bond, could reduce the protonation capacity of the nitrogen. None of the snapshots throughout the MD simulations showed, however, such a structure either in the gas phase or in the aqueous solution. Such a conformation would impose a strong structural restraint on the molecule and could be conceivable only in the gas phase. Hydrogen bond formation is much easier with a water molecule in aqueous solution. Thus, in the absence of a returning side chain that reduces the accessibility of the tertiary nitrogen by water molecules, the pK_a of 8.27 vs 8.44 appears to reflect small changes in the electron structure of the two molecules. The results also suggest that only small deviations from the pK_a of 8.27 are expected for monoamines in this series with different end groups.

Summary. Compound **11** displays an interesting activity profile with agonist activity at M_1 , M_2 , and M_4 receptors. The pharmacological profile suggests potential utility in the treatment of psychiatric disorders including schizophrenia. Compound **11** displays a very low side effect profile in preliminary pharmacological studies in mice, consistent with its lack of activity at M_3 receptors in biochemical assays. Compound **11** does exhibit robust activity at M_2 receptors, which may result in cardiovascular side effects in clinical studies. It remains unclear, however, whether M_2 receptor activity is desirable for antipsychotic activity. Further studies are necessary to optimize the pharmacological properties of the novel series of compounds for the treatment of schizophrenia. Molecular modeling studies revealed that monocationic bivalent ligands with neutral and polar end groups take similar effective lengths as characterized by the $N \cdots O_5$ distance as compared with the dicationic (α,ω -di-tetrahydropyridyl-thiadiazole) ligand. The flexibility of the spacer of the present monocationic ligands increases when the molecules leave the fluid in the synaptic cleft and penetrate into the receptor binding pocket. Upon replacement of the (neutral) polar end group by an apolar moiety (ethyl), the effective length is considerably increased. This structural feature can be usefully considered in designing new derivatives with optimal effective length and flexibility. Ultimately, derivatives of compound **11** may be useful in treating psychosis and cognitive deficits associated with schizophrenia.

Experimental Section

Chemistry. Reactions were carried out under nitrogen. Melting points were determined on a Fisher-Johns melting point apparatus and are presented uncorrected. 1H and ^{13}C NMR spectra were obtained with a Bruker ACF 300 MHz spectrometer. Elemental analyses (C, H, N) were performed by Atlantic Microlab, Inc., GA; analytical results were within $\pm 0.4\%$ of the theoretical values for the formula given unless otherwise indicated. Precoated silica gel GHLF UNIPLATES (250 μm) purchased from Analtech, Inc., DE, were used for thin-layer chromatography, and spots were examined with UV light at 254 nm or with iodine vapor. Column chromatography purification was performed on Davisil silica gel (200–425 mesh) obtained from Fisher Scientific. THF was dried over

sodium-benzophenone ketyl and distilled. All other commercially available solvents and reagents were used without further purification unless otherwise specified.

Compound 7c. A suspension of 60% NaH in mineral oil (1 g, 25.23 mmol) was washed with anhydrous hexane (10 mL) and suspended in freshly distilled THF (30 mL). Then, **7b** (4 mL, 22.94 mmol) was added to the above suspension and the reaction mixture was refluxed for 1 h. After the mixture was cooled to 0 °C using an ice bath, bromoethane (0.88 mL, 11.47 mmol) was added slowly, and the reaction mixture was kept at 0 °C for 1 h. The solvent was evaporated under a vacuum, ice water was added, and then, the aqueous solution was extracted twice with CHCl₃. The combined extract was washed with brine, dried over anhydrous Na₂SO₄, and concentrated to yield the crude compound. After silica gel chromatography (4% CH₃OH in CHCl₃ as eluting solvent), **7c** was obtained (650 mg, as a colorless oil, 25.5% yield); *R_f* = 0.50 (2% CH₃OH in CHCl₃). ¹H NMR (CDCl₃): δ 1.17 (t, 3H), 2.75 (t, 1H, -OH), 3.50 (q, 2H), 3.54–3.71 (m, 16H). ¹³C NMR (CDCl₃): δ 15.1, 61.5, 66.5, 69.7, 70.3, 70.5, 70.6, 72.6.

Compound 12. A suspension of 60% NaH in mineral oil (800 mg, 20 mmol) was washed with anhydrous hexane (10 mL), and then, anhydrous methanol (20 mL) was added under an ice bath. The resulting suspension was refluxed for 1 h before being transferred to an addition funnel. Under an ice bath, the above sodium methoxide suspension was added slowly to a solution of **29** (3.196 g, 20 mmol) in THF (20 mL), and the reaction mixture was maintained at room temperature for 24 h. The mixture was evaporated under a vacuum and quenched with ice water (20 mL), and then, the aqueous solution was extracted with hexane three times. The combined extracts were washed with water, dried over anhydrous Na₂SO₄, and concentrated to yield the crude compound. After silica gel chromatography (hexane, then 5% CH₃OH/CHCl₃ as eluting solvents), **12** was obtained (305 mg, as a white powder, 10.1% yield); mp 52.5–53.5 °C (sublimated); *R_f* = 0.40 (hexane). ¹H NMR (CDCl₃): δ 4.15 (s, -OCH₃). ¹³C NMR (CDCl₃): δ 58.4, 133.3, 160.4.

Preparation of Mono[3-(pyrid-3-yl)-1,2,5-thiadiazol-4-yl]ether Derivatives. General Procedure. Compound 8. A suspension of 60% NaH in mineral oil (560 mg, 14 mmol) was washed with anhydrous hexane (10 mL) and suspended in freshly distilled THF (20 mL). Then, **6** (1.012 g, 5 mmol) was added to the above suspension and the reaction mixture was refluxed for 1 h. Compound **5** (400 mg, 2 mmol) in THF (20 mL) was added, and the reaction mixture was refluxed for 24 h. The mixture was evaporated under a vacuum and quenched with ice water (20 mL). After adjusting the pH < 7, the aqueous solution was extracted twice with CHCl₃. The combined extract was washed with water, dried over anhydrous Na₂SO₄, and concentrated to yield the crude compound. After silica gel chromatography (25–50% EtOAc/hexane as eluting solvent), **8** was obtained (450 mg, as a white powder, 61.9% yield); *R_f* = 0.63 (50% EtOAc in hexane). ¹H NMR (CDCl₃): δ 1.25–1.56 (m, 18H), 1.86 (m, 2H), 2.30 (m, 1H, -OH), 3.61 (t, 2H, -CH₂OH), 4.49 (t, 2H, -OCH₂-), 7.38 (m, 1H), 8.41 (d, 1H, *J* = 6.5 Hz), 8.62 (d, 1H, *J* = 4.6 Hz), 9.37 (s, 1H). ¹³C NMR (CDCl₃): δ 25.9, 26.1, 29.0, 29.4, 29.5, 29.6, 33.0, 63.0, 71.6, 123.6, 127.9, 134.9, 145.1, 148.7, 150.2, 163.0.

Tri(ethylene glycol) Ethyl[3-(pyrid-3-yl)-1,2,5-thiadiazol-4-yl]ether (9a). Compound **9a** was prepared from **7a** (750 mg, 4 mmol) and **5** (200 mg, 1 mmol) using a similar procedure described earlier to afford the title compound **9a** (300 mg, as a brown oil, 88.4% yield); *R_f* = 0.56 (2.5% CH₃OH in CHCl₃). ¹H NMR (CDCl₃): δ 1.14 (t, 3H), 3.50 (q, 2H), 3.53–3.70 (m, 8H), 3.90 (t, 2H), 4.64 (t, 2H), 7.35 (m, 1H), 8.40 (d, *J* = 8.0 Hz, 1H), 8.59 (dd, *J* = 1.6 and 4.8 Hz, 1H), 9.35 (s, 1H).

Compound 9b. Compound **9b** was prepared from **7b** (10.1 mmol) and **5** (500 mg, 2.53 mmol) using a similar procedure described earlier to afford the title compound **9b** (375 mg, as a pale yellow oil, 41.7% yield); *R_f* = 0.60 (10% CH₃OH in CHCl₃). ¹H NMR (CDCl₃): δ 3.57–3.75 (m, 12H), 3.95 (t, 2H), 4.70 (t, 2H), 7.41 (m, 1H), 8.44 (d, *J* = 8.1 Hz, 1H), 8.65 (dd, *J* = 1.6 and 4.8 Hz, 1H), 9.40 (s, 1H). ¹³C NMR (CDCl₃): δ

61.9, 69.4, 70.5, 70.6, 70.8, 70.9, 71.0, 72.7, 123.7, 127.8, 135.2, 145.3, 148.8, 150.3, 162.7.

Tetra(ethylene glycol) Ethyl[3-(pyrid-3-yl)-1,2,5-thiadiazol-4-yl]ether (9c). Compound **9c** was prepared from **7c** (336 mg, 1.5 mmol) and **5** (100 mg, 0.5 mmol) using a similar procedure described earlier to afford the title compound **9c** (185 mg, as a yellow brown oil, 95.3% yield); *R_f* = 0.63 (5% CH₃OH in CHCl₃). ¹H NMR (CDCl₃): δ 1.58 (t, 3H), 3.50 (q, 2H), 3.53–3.70 (m, 12H), 3.90 (t, 2H), 4.65 (t, 2H), 7.36 (m, 1H), 8.41 (d, *J* = 8.0 Hz, 1H), 8.61 (dd, *J* = 1.6 and 4.8 Hz, 1H), 9.36 (s, 1H). ¹³C NMR (CDCl₃): δ 15.3, 66.7, 69.3, 69.9, 70.7, 70.8, 70.9, 123.5, 127.6, 134.8, 145.2, 148.9, 150.3, 162.6.

1-(3-Methoxy-1,2,5-thiadiazol-4-yloxy)-12-[3-(pyrid-3-yl)-1,2,5-thiadiazol-4-yloxy]dodecane (13). A suspension of 60% NaH in mineral oil (80 mg, 2 mmol) was washed with anhydrous hexane (10 mL) and suspended in freshly distilled THF (20 mL). Then, **8** (182 mg, 0.5 mmol) in 20 mL of THF was added to the above suspension. The reaction mixture was refluxed for 30 min. Compound **12** (61 mg, 0.4 mmol) in THF (20 mL) was added, and the reaction mixture was refluxed for 24 h. The mixture was evaporated under a vacuum and quenched with ice water (20 mL), and then, the aqueous solution was extracted twice with CH₂Cl₂. The combined extract was washed with water, dried over anhydrous Na₂SO₄, and concentrated to yield the crude compound. After silica gel chromatography (25% EtOAc in hexane as eluting solvent), **13** was obtained (80 mg, as a pale yellow oil, 41.9% yield); *R_f* = 0.44 (50% EtOAc in hexane). ¹H NMR (CDCl₃): δ 1.27–1.50 (m, 16H), 1.76–1.92 (m, 4H), 4.08 (s, 3H, -OCH₃), 4.37 (t, 2H), 4.50 (t, 2H), 7.38 (m, 1H), 8.41 (d, *J* = 8.0 Hz, 1H), 8.64 (s, 1H), 9.40 (s, 1H). ¹³C NMR (CDCl₃): δ 25.9, 26.1, 29.0, 29.1, 29.4, 29.6, 57.6, 71.0, 71.6, 123.6, 127.8, 134.8, 145.1, 148.8, 150.3, 152.0, 152.5, 163.0.

Tetra(ethylene glycol) (3-Methoxy-1,2,5-thiadiazol-4-yl)[3-(pyrid-3-yl)-1,2,5-thiadiazol-4-yl]ether (14). Compound **14** was prepared from **9b** (355.4 mg, 1.0 mmol) and **12** (180.7 mg, 1.2 mmol) using a similar procedure described in the synthesis of **13** to afford the title compound **14** (125 mg, as a yellow oil, 26.6% yield); *R_f* = 0.60 (5% CH₃OH in CH₂Cl₂). ¹H NMR (CDCl₃): δ 3.65–3.72 (m, 8H), 3.84 (t, 2H), 3.93 (t, 2H), 4.06 (s, 3H, -OCH₃), 4.53 (t, 2H), 4.67 (t, 2H), 7.39 (m, 1H), 8.43 (d, *J* = 8.1 Hz, 1H), 8.63 (dd, *J* = 1.6 and 4.8 Hz, 1H), 9.38 (s, 1H). ¹³C NMR (CDCl₃): δ 57.6, 69.2, 69.3, 69.9, 70.4, 70.9, 123.6, 127.7, 134.9, 145.3, 148.9, 150.3, 151.7, 152.5, 162.7.

Preparation of Mono[3-(1-methylpyridinium-3-yl)-1,2,5-thiadiazol-4-yl]ether Iodides. General Procedure. 12-[3-(1-Methylpyridinium-3-yl)-1,2,5-thiadiazol-4-yloxy]-1-dodecanol Iodide (15). To a solution of **8** (100 mg, 0.275 mmol) in acetone (5 mL) and CHCl₃ (5 mL) was added CH₃I (3 mL, 48 mmol), and the solution was stirred under nitrogen for 36–48 h at room temperature. The residual quaternary iodide **15** was obtained by removing the solvents under reduced pressure and then recrystallized in acetone/ether (136 mg, as a pale yellow-white powder, 97.8% yield); mp 107–109 °C. ¹H NMR (CDCl₃): δ 1.30–1.58 (m, 18H), 1.95 (m, 2H), 3.64 (m, 2H, -CH₂OH), 4.62 (t, 2H, -OCH₂-), 4.81 (s, 3H, -NCH₃), 8.25 (m, 1H), 9.16 (d, *J* = 8.4 Hz, 1H), 9.39 (s, 1H), 9.71 (d, *J* = 5.9 Hz, 1H).

1-(3-Methoxy-1,2,5-thiadiazol-4-yloxy)-12-[3-(1-methylpyridinium-3-yl)-1,2,5-thiadiazol-4-yloxy]dodecane Iodide (16). Compound **16** was prepared from **13** (80 mg, 0.17 mmol) and CH₃I (1 mL, 16 mmol) using a similar procedure described earlier to afford the quaternary iodide **16** (85 mg, as a yellow powder, 81.8% yield); mp 112–113 °C. ¹H NMR (CDCl₃): δ 1.30–1.45 (m, 16H), 1.83 (m, 2H), 1.95 (m, 2H), 4.11 (s, 3H, -OCH₃), 4.40 (t, 2H), 4.61 (t, 2H), 4.82 (s, 3H, -NCH₃), 8.26 (m, 1H), 9.15 (d, *J* = 8.4 Hz, 1H), 9.41 (s, 1H), 9.70 (d, *J* = 6.0 Hz, 1H). ¹³C NMR (CDCl₃): δ 25.9, 26.1, 29.0, 29.4, 29.6, 29.7, 50.9, 57.7, 71.1, 72.7, 128.8, 131.7, 139.6, 142.1, 143.0, 146.0, 152.0, 152.6, 163.4.

Tri(ethylene glycol) Ethyl[3-(1-methylpyridinium-3-yl)-1,2,5-thiadiazol-4-yl]ether Iodide (17a). Compound **17a** was prepared from **9a** (300 mg, 0.88 mmol) and CH₃I (3 mL,

48 mmol) using a similar procedure described earlier to afford the quaternary iodide **17a** (425 mg, as a yellow oil, 99.7% yield). ¹H NMR (DMSO-*d*₆): δ 1.05 (t, 3H), 3.48–3.3.54 (q, 2H), 3.55–3.3.75 (m, 8H), 3.90 (t, 2H), 4.45 (s, 3H, –NCH₃), 4.67 (t, 2H), 8.29(m, 1H), 9.07 (m, 2H), 9.51(s, 1H). ¹³C NMR (DMSO-*d*₆): δ 15.0, 48.5, 65.5, 68.1, 69.1, 69.8, 70.8, 128.0, 130.2, 141.2, 142.6, 143.3, 146.0, 162.5.

Tetra(ethylene glycol) Mono[3-(1-methylpyridinium-3-yl)-1,2,5-thiadiazol-4-yl]ether Iodide (17b). Compound **17b** was prepared from **9b** (100 mg, 0.28 mmol) and CH₃I (1.5 mL, 24 mmol) using a similar procedure described earlier to afford the quaternary iodide **17b** (128 mg, as a yellow oil, 91.5% yield). ¹H NMR (CDCl₃): δ 3.10 (m, 1H, –OH), 3.53–3.79 (m, 2H), 3.99 (t, 2H), 4.74 (t, 2H), 4.81 (s, 3H, –NCH₃), 8.32 (m, 1H), 9.16 (d, *J* = 8.3 Hz, 1H), 9.51(s, 1H), 9.70 (d, *J* = 6.0 Hz, 1H). ¹³C NMR (CDCl₃): δ 50.6, 61.4, 68.9, 70.2, 70.6, 70.7, 70.8, 70.9, 128.9, 131.4, 140.2, 142.7, 143.2, 146.1, 162.8.

Tetra(ethylene glycol) Ethyl[3-(1-methylpyridinium-3-yl)-1,2,5-thiadiazol-4-yl]ether Iodide (17c). Compound **17c** was prepared from **9c** (185 mg, 0.48 mmol) and CH₃I (2 mL, 32 mmol) using a similar procedure described earlier to afford the quaternary iodide **17c** (243 mg, as a yellow oil, 95.9% yield). ¹H NMR (CDCl₃): δ 1.17 (t, 3H), 3.48–3.3.54 (q, 2H), 3.55–3.3.75 (m, 12H), 4.00 (t, 2H), 4.73 (t, 2H), 4.79 (s, 3H, –NCH₃), 8.28(m, 1H), 9.14 (d, *J* = 8.3 Hz, 1H), 9.55(s, 1H), 9.57 (d, *J* = 6.0 Hz, 1H). ¹³C NMR (CDCl₃): δ 15.3, 50.7, 66.9, 69.9, 70.7, 70.8, 71.0, 128.8, 131.5, 140.0, 142.6, 143.3, 146.0, 162.9.

Tetra(ethylene glycol) (3-Methoxy-1,2,5-thiadiazol-4-yl)[3-(1-methyl-pyridinium-3-yl)-1,2,5-thiadiazol-4-yl]ether Iodide (18). Compound **18** was prepared from **14** (125 mg, 0.27 mmol) and CH₃I (1 mL, 16 mmol) using a similar procedure described earlier to afford the quaternary iodide **18** (160 mg, as a yellow oil, 98.4% yield). ¹H NMR (CDCl₃): δ 3.58–3.3.66 (m, 6H), 3.69 (m, 2H), 3.76 (m, 2H), 3.93 (m, 2H), 4.00 (s, 3H, –OCH₃), 4.43 (t, 2H), 4.67 (t, 2H), 4.70 (s, 3H, –NCH₃), 8.23 (m, 1H), 9.09 (d, *J* = 8.3 Hz, 1H), 9.40 (d, *J* = 6.0 Hz, 1H), 9.52 (s, 1H). ¹³C NMR (CDCl₃): δ 50.5, 57.6, 68.8, 69.0, 69.7, 70.4, 70.6, 70.8, 128.7, 131.3, 139.9, 142.5, 143.2, 145.6, 151.4, 152.2, 162.7.

Preparation of Mono[3-(1-methyl-1,2,5,6-tetrahydro-pyrid-3-yl)-1,2,5-thiadiazol-4-yl]ether Hydrochlorides. General Procedure. **12-[3-(1-Methyl-1,2,5,6-tetrahydro-pyrid-3-yl)-1,2,5-thiadiazol-4-yloxy]-1-dodecanol Hydrochloride (23) (CDD-0297-A).** The pyridinium iodide **15** (100 mg, 0.198 mmol) was dissolved in a mixture of CH₃OH (10 mL) and CHCl₃ (10 mL). The solution was cooled to 0–5 °C, and NaBH₄ (30 mg, 0.792 mmol) was added. After the mixture was stirred at 0–5 °C for 2 h, another 30 mg of NaBH₄ was added. The reaction continued for 2 h. Ice water was added to the reaction mixture, which was then extracted twice with CHCl₃. The combined organic extract was washed with water and dried over anhydrous Na₂SO₄. The solvent was removed under reduced pressure, and the residue was chromatographed on a column of silica gel using CHCl₃–CH₃OH (95:5) as eluent. The purified free base **19** was redissolved in a mixture of CH₃OH/CHCl₃ (10 mL, 5:5) and was cooled to 0 °C. Then, dry HCl gas was bubbled through the solution for 3 min, and the title compound **23** was recrystallized from methanol/ether (61.5 mg, as a white powder, 72.7% yield); mp 97–98 °C; free base *R*_f = 0.69 [CHCl₃/CH₃OH (90:10)]. ¹H NMR (D₂O): δ 1.01–1.23 (m, 18H), 1.63 (m, 2H), 2.53 (m, 2H), 2.84 (s, 3H, –NCH₃), 3.27 (m, 4H), 4.03 (m, 2H), 4.22 (m, 2H), 7.03 (s, 1H, vinylic). ¹³C NMR (CDCl₃): δ 22.6, 25.7, 25.9, 28.8, 29.1, 29.4, 32.8, 43.1, 49.7, 51.7, 63.0, 71.4, 123.7, 126.6, 143.9, 162.5. Anal. (C₂₀H₃₅N₃O₂S₁·HCl·0.5H₂O) C, H, N.

12-[3-(1-Methyl-1,2,5,6-tetrahydropyrid-3-yl)-1,2,5-thiadiazol-4-yloxy]-1-dodecyl Acetate Hydrochloride (25) (CDD-0299-A). Compound **25** was prepared from **15** (120 mg, 0.237 mmol) using a similar procedure described earlier to afford the free base **19** (60 mg yellow oil, 66.3% yield); *R*_f = 0.69 [CHCl₃/CH₃OH (90:10)]. ¹H NMR (CDCl₃): δ 1.27–1.57 (m, 18H), 1.87 (m, 2H), 1.95 (m, 2H), 2.45 (s, 3H, –NCH₃), 2.57 (t, 2H), 3.45 (m, 2H), 3.60 (t, 2H), 4.44 (t, 2H), 7.07 (s,

1H, vinylic). ¹³C NMR (CDCl₃): δ 25.9, 26.1, 26.7, 29.0, 29.3, 29.6, 29.7, 33.0, 46.1, 51.4, 55.2, 63.2, 71.1, 128.5, 129.5, 162.8.

The above free base (**19**) was redissolved in acetic anhydride (6 mL, redistilled), and ZnCl₂ powder (10 mg, freshly dried in a vacuum oven for 4 days) was added. Then, the reaction mixture was maintained in an oil bath at 85 °C for 3 h. Ice was added to quench the reaction. The aqueous solution was extracted twice with CHCl₃. The combined organic extract was washed with 10% K₂CO₃ (50 mL) and then water and dried over anhydrous Na₂SO₄. The solvent was removed under reduced pressure, and the residue was chromatographed on a column of silica gel using CHCl₃–CH₃OH (97.5:2.5) as eluent. The purified free base of the ester (**27**) was redissolved in anhydrous CH₂Cl₂ (5 mL) and was cooled to 0 °C. Then, 1 M HCl/ether (1 mL) was added, and the flask was kept at 0 °C for 5 min. The title compound **25** was recrystallized from acetone/ether (53.4 mg, as a hygroscopic yellow-white powder, 48.0% yield); mp 85–86 °C; free base *R*_f = 0.45 [CHCl₃/CH₃OH (95:5)]. ¹H NMR (CDCl₃): δ 1.28–1.43 (m, 18H), 1.62 (m, 2H), 1.72 (m, 2H), 2.05 (s, 3H, acetyl), 2.59 (m, 1H), 2.97 (s, 3H, –NCH₃), 3.25 (m, 1H), 3.57 (m, 1H), 3.78 (m, 1H), 4.05 (t, 2H), 4.46 (t, 2H), 7.27 (s, 1H, vinylic). ¹³C NMR (CDCl₃): δ 21.2, 23.0, 26.1, 28.8, 29.0, 29.4, 29.7, 43.5, 52.2, 64.8, 71.7, 124.0, 126.9, 144.1, 162.7, 171.4. Anal. (C₂₂H₃₇N₃O₃S₁·HCl·0.5H₂O) C, H, N.

1-(3-Methoxy-1,2,5-thiadiazol-4-yloxy)-12-[3-(1-methyl-1,2,5,6-tetrahydro-pyrid-3-yl)-1,2,5-thiadiazol-4-yloxy]-dodecane Hydrochloride (10) (CDD-0308-A). Compound **10** was prepared from **16** (85 mg, 0.237 mmol) using a similar procedure described earlier to afford the title compound **10** (50 mg, as a pale yellow powder, 65.3% yield); mp 108–109 °C; free base *R*_f = 0.33 [EtOAc/hexane (50:50)]. ¹H NMR (CDCl₃): δ 1.19–1.29 (m, 16H), 1.42 (m, 4H), 2.58 (m, 1H), 2.96 (s, 3H, –NCH₃), 2.96 (m, 1H), 3.27 (m, 1H), 3.50 (m, 1H), 3.77 (m, 1H), 4.11 (s, 3H, –OCH₃), 4.37–4.53 (m, 5H), 7.27 (s, 1H, vinylic), 13.1 (s, 1H). ¹³C NMR (CDCl₃): δ 22.8, 26.0, 26.1, 29.0, 29.5, 29.7, 43.3, 50.0, 52.0, 57.7, 71.1, 71.7, 124.0, 126.9, 144.1, 152.0, 152.6, 162.8. Anal. (C₂₃H₃₇N₃O₃S₂·HCl·1.5H₂O) C, H, N.

Tri(ethylene glycol) Ethyl[3-(1-methyl-1,2,5,6-tetrahydropyrid-3-yl)-1,2,5-thiadiazol-4-yl]ether Hydrochloride (24a) (CDD-0282-A). Reduction of the pyridinium iodide **17a** (420 mg, 0.87 mmol) yielded the hydrochloride **24a** (180 mg, as a yellow hygroscopic solid, 51.3% yield); mp: 75–76 °C; free base *R*_f = 0.53 [CHCl₃/CH₃OH (95:5)]. ¹H NMR (D₂O): δ 0.95 (t, 3H), 2.53 (m, 2H), 2.85 (s, 3H, –NCH₃), 3.10 (m, 1H), 3.35 (m, 1H), 3.44–3.57 (m, 10H), 3.80 (m, 2H), 3.87 (m, 1H), 4.25 (m, 1H), 4.46 (m, 2H), 7.06 (s, 1H, vinylic). Anal. (C₁₆H₂₇N₃O₄S₁·HCl·0.5H₂O) C, H, N.

Tetra(ethylene glycol) Mono[3-(1-methyl-1,2,5,6-tetrahydropyrid-3-yl)-1,2,5-thiadiazol-4-yl]ether Hydrochloride (24b) (CDD-0300-A). Reduction of the pyridinium iodide **17b** (120 mg, 0.24 mmol) yielded the hydrochloride **24b** (75.7 mg, as a pale yellow oil, 76.9% yield); free base *R*_f = 0.38 [CHCl₃/CH₃OH (90:10)]. ¹H NMR (CDCl₃): δ 2.56–2.62 (m, 2H), 2.95 (s, 3H, –NCH₃), 3.03 (m, 1H), 3.55–3.82 (m, 14H), 3.90 (m, 2H), 4.50 (m, 1H), 4.63 (m, 2H), 7.30 (s, 1H, vinylic). ¹³C NMR (CDCl₃): δ 22.8, 43.3, 50.0, 51.9, 61.9, 69.3, 70.3, 70.5, 70.9, 72.7, 123.7, 127.5, 144.3, 162.4. Anal. (C₁₆H₂₇N₃O₅S₁·HCl·0.5H₂O) C, H, N.

Tetra(ethylene glycol) Ethyl[3-(1-methyl-1,2,5,6-tetrahydropyrid-3-yl)-1,2,5-thiadiazol-4-yl]ether Hydrochloride (24c) (CDD-0301-A). Reduction of the pyridinium iodide **17c** (243 mg, 0.46 mmol) yielded the hydrochloride **24c** (93 mg, as a pale white powder, 46.2% yield); mp 64.5–66 °C; free base *R*_f = 0.49 [CHCl₃/CH₃OH (95:5)]. ¹H NMR (CDCl₃): δ 1.20 (t, 3H), 2.58 (m, 1H), 2.95 (s, 3H, –NCH₃), 3.03 (m, 1H), 3.23 (m, 1H), 3.47–3.88 (m, 16H), 3.90 (m, 2H), 4.48 (m, 1H), 4.62 (m, 2H), 7.29 (s, 1H, vinylic), 13.1 (s, 1H). ¹³C NMR (CDCl₃): δ 15.4, 22.7, 43.2, 49.9, 51.9, 66.8, 69.3, 70.0, 70.3, 70.8, 123.7, 127.4, 144.3, 162.4. Anal. (C₁₈H₃₁N₃O₅S₁·HCl·0.5H₂O) C, H, N.

Tetra(ethylene glycol) Mono[3-(1-methyl-1,2,5,6-tetrahydropyrid-3-yl)-1,2,5-thiadiazol-4-yl]ether Acetate Hydrochloride (26) (CDD-0303-A). Reduction of **17b** (100 mg, 0.20 mmol) yielded the free base **21b** (40 mg, as a yellow oil,

53.6% yield); $R_f = 0.31$ [$\text{CHCl}_3/\text{CH}_3\text{OH}$ (90:10)]. The above free base was treated with acetic anhydride (4 mL) and ZnCl_2 powder (10 mg) following the similar procedure as described in the synthesis of compound **25** to afford the title compound **26** (35.5 mg, as a yellow-white powder, 36.3% yield); mp 55–55.5 °C (hygroscopic); free base $R_f = 0.48$ [$\text{CHCl}_3/\text{CH}_3\text{OH}$ (90:10)]. ^1H NMR (CDCl_3): δ 2.07 (s, 3H, acetyl), 2.58 (m, 1H), 2.95 (s, 3H, $-\text{NCH}_3$), 2.96 (m, 1H), 3.20 (m, 1H), 3.56 (m, 1H), 3.66–3.71 (m, 12H), 3.80 (m, 1H), 3.90 (t, 2H), 4.48 (m, 1H), 4.62 (t, 2H), 7.29 (s, 1H, vinylic), 13.1 (s, 1H). ^{13}C NMR (CDCl_3): δ 21.2, 22.9, 43.4, 50.0, 52.0, 63.7, 69.3, 70.3, 70.8, 70.9, 123.7, 127.4, 144.3, 162.4, 171.2. Anal. ($\text{C}_{18}\text{H}_{29}\text{N}_3\text{O}_6\text{S}_1 \cdot \text{HCl} \cdot 0.5\text{H}_2\text{O}$) C, H, N.

Tetra(ethylene glycol) (3-Methoxy-1,2,5-thiadiazol-4-yl)[3-(1-methyl-1,2,5,6-tetrahydropyrid-3-yl)-1,2,5-thiadiazol-4-yl]ether Hydrochloride (11) (CDD-0304-A). Reduction of the pyridinium iodide **18** (160 mg, 0.26 mmol) yielded the hydrochloride **11** (23 mg, as a hygroscopic pale yellow powder, 16.1% yield); mp 35–37 °C; free base $R_f = 0.70$ [$\text{CH}_2\text{Cl}_2/\text{CH}_3\text{OH}$ (95:5)]. ^1H NMR (CDCl_3): δ 2.62 (m, 2H), 2.95 (m, 5H), 3.23 (m, 2H), 3.55 (m, 2H), 3.69 (m, 6H), 3.89 (m, 4H), 4.10 (s, 3H), 4.56 (t, 2H), 4.63 (m, 2H), 7.30 (s, 1H). ^{13}C NMR (CDCl_3): δ 22.9, 43.5, 50.1, 52.0, 57.7, 69.3, 70.0, 70.4, 70.9, 71.0, 123.7, 127.4, 144.3, 151.7, 152.6, 162.4. Anal. ($\text{C}_{19}\text{H}_{29}\text{N}_5\text{O}_6\text{S}_2 \cdot \text{HCl} \cdot \text{H}_2\text{O}$) C, H, N.

Determination of Protonation Constants. The standard potentiometric method (temperature, 25.0 ± 0.1 °C; ionic strength, 0.15 M KCl; N_2 atmosphere) and the $\text{GLP}K_a$ automated instrument (Sirius Anal. Ltd., U.K.) were used for the determination of protonation constants of the samples. The details of the experiments are the same as published previously.¹⁷ Five separate measurements were carried out, and the average pK_a values along with the standard deviations were calculated.

Pharmacology. Mouse fibroblast (A9 L) cells and CHO cells were purchased from American Type Culture Collection (ATCC) (Rockville, MD). Dulbecco's modified Eagle media (DMEM), l-glutamine solution, penicillin/streptomycin solution, trypsin, geneticin (G-418 Sulfate Solid), 3-isobutyl-1-methylxanthine (IBMX), and all other inorganic chemicals were purchased from Fisher Scientific Company L. L. C. (Hanover Park, IL). Fetal bovine serum was purchased from EQUITECH-BIO, Inc. (Kerrville, TX). Bovine serum albumin, atropine-sulfate, carbamylcholine chloride (carbachol), trichloroacetic acid, and Triton X-100 were purchased from Sigma-Aldrich Co. (St. Louis, MO). Opti-MEM I reduced-serum media and MEM nonessential amino acids solution were purchased from Life Technologies, Inc. (Gaithersburg, MD). Forskolin and UniverSol ES scintillation cocktail were bought from ICN Biomedicals, Inc. (Irvine, CA). MicroScint 20 was purchased from PerkinElmer Life Science (Boston, MA). Both *myo*-[2- ^3H]-inositol (10–25 Ci/mmol) and [^3H]-(*R*)-QNB (30–60 Ci/mmol) were purchased from NEN Life Science Products, Inc. (Boston, MA). The QIAGEN endofree plasmid Maxi kit was bought from QIAGEN Inc. (Valencia, CA). LipofectAMINE 2000 reagent was purchased from Invitrogen (Carlsbad, CA). The direct Cyclic AMP Enzyme Immunoassay Kit was purchased from Assay Designs, Inc. (Ann Arbor, MI).

Receptor Assays. Plasmids for muscarinic receptor subtypes were obtained as a gift from Dr. Tom I. Bonner of the National Institutes of Health. Membrane homogenates were prepared from transfected cells using established procedures.^{18–21} All binding assays were conducted in a 1 mL mixture of binding buffer [25 mM sodium phosphate (pH 7.4) containing 5 mM magnesium chloride]. In saturation binding assays, eight concentrations of [^3H]-(*R*)-QNB were used ranging from 5 to 300 pM. In ligand inhibition binding assays, 0.1 nM [^3H]-(*R*)-QNB and 14 points for the test ligand (ranging from 0.01 nM to 3 mM) were used. The mixture was incubated for 2 h at room temperature. Total binding and nonspecific binding were determined in the absence and presence of 1000-fold excess of unlabeled (*R*)-QNB. Radioactivity was counted using either a 6895 BetaTrac liquid scintillation counter (TM Analytic, Elk Grove Village, IL) or a TopCount NXT system

(Packard, Meriden, CT). Consistent results were obtained from both systems for saturation binding and inhibition binding assays.

The M_1 , M_3 , and M_5 subtypes of muscarinic receptor couple efficiently to phospholipase $C\beta$ via the $G_{q/11}$ family of G proteins. Compounds were examined for their abilities to activate G proteins by measuring accumulation of [^3H]inositol phosphates in stably transfected cells (A9 L cells and/or NIH 3T3 cells) upon agonist stimulation as described previously.¹¹ Cells were transfected with plasmids containing the genes for human M_1 , M_3 , or M_5 receptors (provided by Dr. Tom Bonner of the National Institutes of Health).^{22,23} Activity is presented as the percentage activation above basal levels. Carbachol was utilized in each assay as a positive control for muscarinic receptor activation.

In contrast to the M_1 , M_3 , and M_5 muscarinic receptor subtypes, the M_2 and M_4 receptors signal preferentially through inhibition of the cAMP pathway. Hence, ligands were investigated for their abilities to inhibit forskolin-stimulated cAMP accumulation in cells expressing either human M_2 or M_4 receptors. The Assay Designs Correlate-EIA Direct cyclic AMP kit was used to determine cAMP levels. The day before the experiment, cells were treated with trypsin and seeded into 24 well tissue culture plates with 500 μL of DMEM (without serum) per well and incubated at 37 °C and 5% CO_2 for 16–20 h to about 90% confluence. The media was removed, and cells were treated with 500 μL of DMEM (without serum) containing 300 μM IBMX, 20 μM forskolin, and appropriate ligand concentrations (with DMEM serving as the control). The reaction was terminated after 15 min incubation at 37 °C by aspiration of media and addition of 200 μL 0.1 M HCl. After 10 min, the cells were inspected visually to verify cell lysis and then transferred to Eppendorf tubes and centrifuged at 10 000 rpm at room temperature, and then, the supernatant was used directly in the assay. A polyclonal antibody from the Correlate-EIA Direct cyclic AMP kit was used to bind cAMP. After a simultaneous incubation (2 h) at room temperature, the excess reagents were washed away and substrate was added. After a short incubation time (1 h), the enzyme reaction was stopped and the yellow color generated was read on a microplate reader at 405 nm. The measured optical density was used to calculate the concentration of cAMP.

Pharmacological Screens. Observations of specific behaviors helped determine the incidence of side effects associated with injections of compound **11** and oxotremorine (for comparison). Mice were injected (i.p.) with saline or 0.1 or 1.0 mg/kg of drug dissolved in saline and observed for 2 h according to methods described previously.^{13,24} Three animals received each dose. (A single animal was tested with 10 mg/kg of compound **11**.) Animals were observed over a 10 s interval three times during each of three 30 min periods. Relevant behaviors included salivation, lacrimation, tremors, micturition, diarrhea, grooming, rearing and sniffing, respiratory rate (elevated or depressed), and locomotor behavior. Body temperature also was recorded using a rectal probe. Particular attention was paid toward behaviors associated with muscarinic receptor activity, including hypothermia, salivation, lacrimation, tremors, and diarrhea.

If a behavior was observed during that 10 s period, a score of 1 was given, while 0 was recorded if the behavior did not occur. Scores were averaged for each half hour period and again averaged for the group of three animals at each dose. Thus, a score of 1.0 indicates that all three mice exhibited a particular behavior each time it was observed during a 30 min period. The studies provided an indication of the *in vivo* selectivity and the time course of action for compound **11** as compared with the classical muscarinic agonist oxotremorine.

Ex Vivo Binding Assays. To assess the ability of ligands to cross the blood–brain barrier following peripheral injections, young, male Long-Evans rats were injected with either saline or 0.1 or 1.0 mg/kg of drug in saline intraperitoneally (i.p.) and sacrificed by cervical dislocation at 0.5 and 1.0 h after injection. Brains were removed, and a crude homogenate was prepared from whole brain to be used in *ex vivo* binding

studies. The binding of 1 nM [³H]QNB was assayed using methods outlined previously,^{13,25} including 1000-fold excess of unlabeled atropine to measure nonspecific binding. The ability for each ligand to penetrate the brain was assessed by comparing the level of [³H]QNB binding between saline- and drug-injected animals at each time point. Results were expressed as a percentage of specific [³H]QNB binding to brains of control animals.

Data Analysis. Nonlinear least squares curve fitting was performed using DeltaGraph Pro (DeltaPoint Inc., version 4.0.1) for the Macintosh. Dose–response data were fit to a one site stimulation model to obtain S_{\max} (maximal levels of stimulation), I_{\max} (maximal levels of inhibition), and pEC₅₀ or pIC₅₀ values. Saturation binding data were fit to a one site binding model for B_{\max} and K_d values. Ligand inhibition binding data were fit to one site, two site, and three site binding models. Statistical comparisons between one site and multiple site models were carried out using an *F* test with and α set at the 0.05 level. Then, p*K*_i values were converted from pIC₅₀ values according to the Cheng–Prusoff formula.²⁶ Analysis of variance with posthoc Tukey–Kramer tests were utilized for comparing differences in receptor binding affinity and receptor activation.

Computational Chemistry. Molecular modeling was performed utilizing the Sybyl 6.6 software of Tripos.²⁷ Extended conformations were generated for **24b,c**, **26**, and **11**, and geometries were optimized using the AM1 semiempirical quantum chemical method.²⁸ Atomic charges were obtained from the calculations and implemented in the Tripos force field with a distance-dependent dielectric constant and a 20 Å nonbonded cutoff. MD simulations (130 ps) were performed for all four molecules in the gas phase. The time step was set to 1 fs, and no SHAKE restriction was applied. Each molecule started from an all-trans conformation along the O–CH₂–···–CH₂–O spacer with the torsional angle set to 90° for the central CH₂–CH₂ bond. The molecules rapidly left this conformation at *T* = 310 K and formed generally some sort of a V shape structure, which fluctuated, however, between an almost U and a largely opened V conformation. The last conformation taken at 130 ps in the gas phase was accepted as the starting structure for NpT MD simulations in aqueous solution.

Isothermal–isobaric simulations at *T* = 310 K and *p* = 1 atm mimic natural conditions: the temperature corresponds to that of the human body, and the constant pressure applied leads to reasonable density (near to 1 g/cm³) for the equilibrated solution. A TIP3P water box was used with periodic boundary conditions and with a nonbonded cutoff of 8 Å. A chloride counterion was added to the system and set to 6–7 Å apart from the proton of the tetrahydropyridyl ring in the starting solution structure. Utilization of the SHAKE option for single bonds allowed a time step of 2 fs. A 250 ps equilibration phase was followed by another 250 ps simulation period used for structure analysis. In calculations with three NaCl molecules in the system, the isotonic saline concentration (0.153 M) was mimicked with about 1300 TIP3P water molecules in the water box. The simulations, using the same parameters as described previously, were performed for **11** with a 250 ps simulation time for each of the equilibration and averaging phases.

Acknowledgment. The work was supported by research grants NS31173 and NS35127 from the National Institutes of Health. We thank Ms. Karen Papadakis for her secretarial assistance in the preparation of the manuscript.

References

- Caulfield, M. P.; Birdsall, N. J. International Union of Pharmacology. XVII. Classification of muscarinic acetylcholine receptors. *Pharmacol. Rev.* **1998**, *50*, 279–290.
- Aboud, L. G.; Biel, J. H. Anticholinergic psychotomimetic agents. *Int. Rev. Neurobiol.* **1962**, *4*, 217–273.
- Cummings, J. L.; Back, C. The cholinergic hypothesis of neuropsychiatric symptoms in Alzheimer's disease. *Am. J. Geriatr. Psychiatry* **1998**, *6*, S64–S78.
- Levy, M. L.; Cummings, J. L.; Kahn-Rose, R. Neuropsychiatric symptoms and cholinergic therapy for Alzheimer's disease. *Gerontology* **1999**, *45* (Suppl. 1), 15–22.
- Cummings, J. L. The role of cholinergic agents in the management of behavioural disturbances in Alzheimer's disease. *Int. J. Neuropsychopharmacol.* **2000**, *3*, 21–29.
- Bodick, N. C.; Offen, W. W.; Shannon, H. E.; Satterwhite, J.; Lucas, R.; van Lier, R.; Paul, S. M. The selective muscarinic agonist xanomeline improves both the cognitive deficits and behavioral symptoms of Alzheimer disease. *Alzheimer Dis. Assoc. Disord.* **1997**, *11*, S16–S22.
- Bodick, N. C.; Offen, W. W.; Levey, A. I.; Cutler, N. R.; Gauthier, S. G.; Satlin, A.; Shannon, M. E.; Tollefson, G. D.; Rasmussen, K.; Bymaster, F. P.; Hurley, D. J.; Potter, W. Z.; Paul, S. M. Effects of xanomeline, a selective muscarinic receptor agonist, on cognitive function and behavioral symptoms in Alzheimer disease. *Arch. Neurol.* **1997**, *54*, 465–473.
- Rasmussen, T.; Fink-Jensen, A.; Sauerberg, P.; Swedberg, M. D.; Thomsen, C.; Sheardown, M. J.; Jeppesen, L.; Calligaro, D. O.; DeLapp, N. W.; Whitesitt, C.; Ward, J. S.; Shannon, H. E.; Bymaster, F. P. The muscarinic receptor agonist BuTAC, a novel potential antipsychotic, does not impair learning and memory in mouse passive avoidance. *Schizophr. Res.* **2001**, *49*, 193–201.
- Friedman, J. I.; Temporini, H.; Davis, K. L. Pharmacologic strategies for augmenting cognitive performance in schizophrenia. *Biol. Psychiatry* **1999**, *45*, 1–16.
- Felder, C. C.; Porter, A. C.; Skillman, T. L.; Zhang, L.; Bymaster, F. P.; Nathanson, N. M.; Hamilton, S. E.; Gomez, J.; Wess, J.; McKinzie, D. I. Elucidating the role of muscarinic receptors in psychosis. *Life Sci.* **2001**, *68*, 2605–2613.
- Rajeshwaran, W. G.; Cao, Y.; Huang, X. P.; Wroblewski, M. E.; Colclough, T.; Lee, S.; Liu, F.; Nagy, P. I.; Ellis, J.; Levine, B. A.; Nocka, K. H.; Messer, W. S., Jr. Design, Synthesis, and Biological Characterization of Bivalent 1-Methyl-1,2,5,6-tetrahydropyridyl-1,2,5-thiadiazole Derivatives as Selective Muscarinic Agonists. *J. Med. Chem.* **2001**, *44*, 4563–4576.
- Sauerberg, P.; Olesen, P. H.; Nielsen, S.; Treppendahl, S.; Sheardown, M. J.; Honore, T.; Mitch, C. H.; Ward, J. S.; Pike, A. J.; Bymaster, F. P.; et al. Novel functional M₁ selective muscarinic agonists. Synthesis and structure–activity relationships of 3-(1,2,5-thiadiazolyl)-1,2,5,6-tetrahydro-1-methylpyridines. *J. Med. Chem.* **1992**, *35*, 2274–2283.
- Messer, J. W. S.; Abuh, Y. F.; Ryan, K.; Shepherd, M. A.; Schroeder, M.; Abunada, S.; Sehgal, R.; El-Assadi, A. A.; Szász, G.; Brann, M. R. Tetrahydropyrimidine derivatives display functional selectivity for M₁ muscarinic receptors in brain. *Drug Dev. Res.* **1997**, *40*, 171–184.
- Jakubik, J.; El-Fakahany, E. E.; Tucek, S. Evidence for a tandem two-site model of ligand binding to muscarinic acetylcholine receptors. *J. Biol. Chem.* **2000**, *275*, 18836–18844.
- CRC Handbook of Chemistry and Physics*, 83rd ed.; CRC Press LLC: Boca Raton, FL, 2002.
- Boudon, S.; Wipff, G. Conformational analysis of protonated ethylenediamine in the gas phase and in water. *J. Mol. Struct. (THEOCHEM)* **1991**, *228*, 61–70.
- Takács-Novák, K.; Noszá, B.; Hermeicz, I.; Keresztúri, G.; Podányi, B.; Abunada, S.; Sehgal, R.; El-Assadi, A. A.; Szász, G.; Brann, M. R. Protonation equilibria of quinolone antibacterials. *J. Pharm. Sci.* **1990**, *79*, 1023–1028.
- Dorje, F.; Wess, J.; Lambrecht, G.; Tacke, R.; Mutschler, E.; Abunada, S.; Sehgal, R.; El-Assadi, A. A.; Szász, G.; Brann, M. R. Antagonist binding profiles of five cloned human muscarinic receptor subtypes. *J. Pharmacol. Exp. Ther.* **1991**, *256*, 727–733.
- Huang, X. P.; Williams, F. E.; Peseckis, S. M.; Messer, W. S., Jr. Pharmacological characterization of human m1 muscarinic acetylcholine receptors with double mutations at the junction of TM VI and the third extracellular domain. *J. Pharmacol. Exp. Ther.* **1998**, *286*, 1129–1139.
- Huang, X. P.; Nagy, P. I.; Williams, F. E.; Peseckis, S. M.; Messer, W. S., Jr. Roles of threonine 192 and asparagine 382 in agonist and antagonist interactions with M₁ muscarinic receptors. *Br. J. Pharmacol.* **1999**, *126*, 735–745.
- Huang, X. P.; Williams, F. E.; Peseckis, S. M.; Messer, W. S., Jr. Differential modulation of agonist potency and receptor coupling by mutations of Ser388Tyr and Thr389Pro at the junction of transmembrane domain VI and the third extracellular loop of human M₁ muscarinic acetylcholine receptors. *Mol. Pharmacol.* **1999**, *56*, 775–783.
- Bonner, T. I.; Buckley, N. J.; Young, A. C.; Brann, M. R. Identification of a family of muscarinic acetylcholine receptor genes. *Science* **1987**, *237*, 527–532.

- (23) Bonner, T. I.; Young, A. C.; Brann, M. R.; Buckley, N. J. Cloning and expression of the human and rat m5 muscarinic acetylcholine receptor genes. *Neuron* **1988**, *1*, 403–410.
- (24) Messer, W. S., Jr.; Bachmann, K. A.; Dockery, C.; El-Assadi, A. A.; Hassoun, E.; Haupt, N.; Tang, B.; Li, X. Development of CDD-0102 as a selective M1 agonist for the treatment of Alzheimer's disease. *Drug Dev. Res.* **2002**, *57*, 200–213.
- (25) Bymaster, F. P.; Heath, I.; Hendrix, J. C.; Shannon, H. E. Comparative behavioral and neurochemical activities of cholinergic antagonists in rats. *J. Pharmacol. Exp. Ther.* **1993**, *267*, 16–24.
- (26) Cheng, Y.; Prusoff, W. H. Relationship between the inhibition constant (K_i) and the concentration of inhibitor which causes 50% inhibition (I_{50}) of an enzymatic reaction. *Biochem. Pharmacol.* **1973**, *22*, 3099–3108.
- (27) *Sybyl*, 6.6 ed.; Tripos, Inc.: St. Louis, MO.
- (28) Dewar, M. J. S.; Zebisch, E. G.; Healy, E. F.; Stewart, J. J. P. AM1: A new general purpose quantum mechanical molecular model. *J. Am. Chem. Soc.* **1985**, *107*, 3902–3909.

JM0301235